Hindawi
Journal of Advanced Transportation
Volume 2022, Article ID 9604362, 17 pages
https://doi.org/10.1155/2022/9604362

Research Article

Train Scheduling Optimization for an Urban Rail Transit Line: A Simulated-Annealing Algorithm Using a Large Neighborhood Search Metaheuristic

Hai Zhang [1,2,3] **and Shaoquan Ni** [1,2,3]

[1]*School of Transportation and Logistics, Southwest Jiaotong University, Chengdu 610031, China*
[2]*National and Local Joint Engineering Laboratory of Comprehensive Intelligent Transportation, Southwest Jiaotong University, Chengdu 610031, China*
[3]*National Engineering Laboratory of Integrated Transportation Big Data Application Technology, Southwest Jiaotong University, Chengdu 610031, China*

Correspondence should be addressed to Hai Zhang; zhzxt666666@126.com

Received 11 August 2022; Revised 10 November 2022; Accepted 28 November 2022; Published 17 December 2022

Academic Editor: Yuan Gao

This paper describes an optimization model for an irregular train schedule. The aim is to optimize both the maximum train loading rate and the average deviation of departure intervals under time-varying passenger transport demand for an urban rail transit line in consideration of practical train operation constraints, i.e., headway, running time between stations, dwell time, and capacity. A heuristic simulated-annealing algorithm is designed to solve the optimization model, and a case study of an urban rail transit line is performed to assess its efficacy. The results show that, compared with the current regular train schedule, the total train dwell time under the optimized irregular schedule is reduced from 900 s to 848 s, and the reduction ratio for the maximum train loading rate is from 1.2% to 3.6% for different stations. When the average train departure interval is allowed to vary from 120 to 170 s, the optimized irregular schedule decreases the maximum train loading rate of the collinear and noncollinear sections by 3.21%–4.82% and 2.52%–3.64%, respectively. Sensitivity analysis is performed for a nonnegative weight coefficient, average train departure interval, and proportion of full-length and short-turn routings. The proposed approach can be used to support capacity improvement and schedule optimization for urban rail transit lines.

1. Introduction

Urban rail transit (URT) is very important for the stability, efficiency, and sustainability of public transportation. As an important target of optimization in railway transportation, train scheduling has received considerable attention. The models designed to generate or optimize train schedules [1–7] can be divided into two different categories: regular and irregular. Unlike irregular train schedules, regular ones are easy for travelers to remember and can be computed with less effort by railway planners [8]. Various optimization models for railway transportation have been proposed to generate periodic timetables that minimize passenger waiting times [9–11]. Odijk [12] used a particular mathematical model to generate periodic timetables, while Liebchen [13] formulated a periodic event-scheduling problem based on a well-established graph model. Shafahi and Khani [14] presented two models with constant headway for minimizing the transfer waiting time in transit networks, and Li and Lo [15] proposed an integrated energy-efficient operation model that jointly optimizes train timetables and speed profiles, thus minimizing energy consumption. Aksu and Akyol [16] proposed a heuristic genetic algorithm (GA) that considers both the operational and transfer costs when creating timetables with homogeneous headways. Yang et al. [17] proposed a cooperative scheduling approach to optimize subway system timetables so that the

recovery energy can be used directly and designed a GA with binary encoding to solve the integer-programming optimization model.

Regular train schedules with a constant headway between consecutive trains reduce passenger waiting times under the condition that the passengers arrive at stations following a uniform or Poisson process [18]. However, regular train schedules may result in longer passenger traveling and waiting times under time-varying passenger transport demand (PTD). Nowadays, with the formation of URT networks, PTD is increasing. When the passenger arrival rate at URT stations is distributed unevenly, regular train schedules are not conducive to matching transport capacity with passenger flow demand, whereas irregular schedules have substantial potential to reduce the total passenger waiting time by matching the actual passenger demand. Therefore, to provide a more efficient timetable that can deal with variable passenger arrival rates, researchers have begun to focus on generating nonfixed-headway train schedules.

Assis et al. [19] proposed a linear-programming model that effectively optimizes train schedules considering time-varying PTD. Guihaire and Hao [20] discussed the scheduling problem in terms of passenger satisfaction and showed that it would be preferable to obtain more detailed data for real-world PTD. Albrecht [21] proposed a multilevel optimization algorithm that produces flexible timetables for a demand-oriented service. Hassannayebi et al. [22] proposed a two-stage GA-based simulation optimization approach to minimize passenger waiting cost for a single-loop URT line, while Sun et al. [23] presented three optimization models for demand-sensitive timetables and found that a dynamic timetable built with capacity constraints offers the greatest ability to reduce the total waiting time. Niu et al. [24] considered train scheduling under time-dependent PTD and train skip-stop patterns and established a unified quadratic integer-programming model that minimizes the total passenger waiting time. Wang et al. [25] proposed an iterative convex programming approach for train scheduling based on time-varying passenger flow, allowing both the total energy consumption and passenger travel time to be minimized. Zhu et al. [26] proposed a bilevel programming model for train-timetable optimization with full consideration of PTD for a URT line. Shi et al. [27] proposed a joint optimization model for collaboratively optimizing the train timetable and passenger flow control strategy for an oversaturated URT line, and Wang et al. [28] proposed three approaches for solving a multiobjective mixed-integer nonlinear programming model to deliver both an irregular train schedule and a rolling-stock circulation plan under time-varying PTD. Xie et al. [29] established a PTD-oriented approach and stop-plan synchronization optimization model that give an energy-saving and stable timetable, whereas Huang et al. [30] developed nonlinear mixed-integer programming models to reschedule trains during disruption, with the purpose of alleviating passenger inconvenience and regaining nominal train regularity. Yin et al. [31] proposed an integrated approach for train scheduling with dynamic PTD on a bidirectional URT line to minimize operational costs and passenger waiting time. Barrena et al. [32] proposed two nonlinear programming formulations for optimizing a rapid-transit timetable under dynamic PTD, with the objective of minimizing the average passenger waiting time at stations. Canca et al. [33] presented a nonlinear integer-programming model for determining noncyclic railway timetables under dynamic PTD, while Chen et al. [34] presented an energy-saving timetable optimization model that minimizes the energy consumption of train stops and the travel time of trains. Meng et al. [35] presented an optimization model and heuristic technique for reallocating the time margins in train timetables so as to minimize train delays under operational disturbances. Barrena et al. [36] presented three linear formulations for timetabling adapted to a dynamic PTD pattern, with the objective of minimizing passenger average waiting time at stations, and developed a branch-and-cut algorithm applicable to all models. Yang et al. [37] presented an integrated biobjective optimization model to generate an irregular timetable, thus enabling the joint optimization of passenger travel time and energy consumption. Dong et al. [38] proposed an integrated optimization model that considers both train stop plans and timetables under time-dependent PTD and showed that the integrated model improved passenger travel efficiency and reduced train running times.

URT has become an important part of urban public transport, offering large-volume transport at fast speeds with high levels of punctuality. Compared with other public transport methods, URT is a closed operating environment with high passenger density. Since the outbreak of COVID-19, the difficulties in controlling the spread of epidemics have increased. To reduce the risk of epidemic transmission, reducing the train loading rate is now required for epidemic normalization and control in China. In this paper, under the premise of a certain average train departure interval, the capacities of irregular trains are accurately determined via an optimized train schedule to reduce the maximum train loading rate. Previous studies of irregular train timetables have not accounted for the negative impact of unbalanced train departure intervals on passengers. If the train departure intervals are too uneven, there will be an excessive imbalance in waiting times, which will make it difficult for passengers to adapt and will increase the complexity of preparing and operating train timetables. Therefore, this paper presents an optimization model for an irregular train schedule during peak hours. The model achieves the cooperative optimization of the maximum train loading rate and equilibrium of train departure intervals, thus improving the passenger experience.

The remainder of this paper is structured as follows: in Section 2, the problem and related assumptions are presented, and an optimization model for minimizing the maximum train loading rate and the average deviation of train departure intervals is described. In Section 3, the solution approach for the optimization model is introduced. Section 4 evaluates the performance of the proposed model through a case study. Finally, the conclusions to this study and directions for future research are given in Section 5.

2. Problem Description and Model Formulation

2.1. Problem Description. Considering the double-track URT line shown in Figure 1, I platforms are set in each direction, giving a total of $2I$ platforms. Both full-length and short-turn routings are used for train operations, with platform F used for the turn-back operation of short-turn routing. The train turns back before the initial station and after the tail station.

For a traditional regular train schedule, the scheduled running time and dwell time are configured to have the same values for each train. However, a fixed dwell time consumes transport capacity for stations with small passenger flows and often cannot meet the demand for boarding and alighting passengers at stations with large passenger flows, resulting in train delays. This paper correlates the train dwell time with the number of boarding and alighting passengers; see equation (5) in Section 2.5 for details.

As well as the loading rate of train services, passenger satisfaction is influenced by the deviation of train departure intervals. Therefore, this paper constructs an irregular train-scheduling optimization model that jointly optimizes the maximum train loading rate and the average deviation of train departure intervals so as to match passenger demands more accurately.

2.2. Assumptions. Based on the practical operational situation of a URT line, the train-scheduling problem involves the following assumptions:

(1) All the service trains are of the same type and formation.

(2) Each train stops at each station, and there is no overtaking along sections or at stations.

(3) The origin-destination (O-D) matrix of passenger flow demand comes from recent Automatic Fare Collection System (AFC) data. The passenger arrival rate is obtained after sorting, screening, and other related preprocessing.

(4) After all passengers disembark at the turn-back platform, the train starts its turn-back operation.

(5) After each train completes one service in peak hours, it immediately starts the next service rather than returning to the depot.

2.3. Notation and Variables. Table 1 lists the parameters and intermediate variables used in the model, and Table 2 lists the decision variables.

2.4. Objective Function. The optimization objective is to minimize the maximum train loading rate and the average deviation in the train departure interval. The relevant equations are as follows:

$$\min f = 5\lambda\delta_{\max} + (1-\lambda)h_{\Delta}, \tag{1}$$

$$\delta_{\max} = \max\left\{\delta_{k,i}\right\}, \quad \forall k \in K;\ \forall i \in Z, \tag{2}$$

$$h_{\text{ave}} = \frac{\sum_{k=1}^{K}\sum_{i=1}^{2I} h_{k,i}}{K(2I-2)}, \tag{3}$$

$$h_{\Delta} = \frac{\sum_{k=1}^{K}\sum_{i=1}^{2I} \left|h_{k,i} - h_{\text{ave}}\right|}{K(2I-2)}. \tag{4}$$

Equation (1) is the objective function, where λ is a positive weight. In equation (2), $\delta_{\max}$ is the maximum loading rate of all the trains passing through each station. In equation (3), h_{ave} is the average value of the departure intervals of all adjacent trains passing through each station. Equation (4) is the formula for the average deviation of the train departure interval.

2.5. Systematic Constraints. In this subsection, systematic constraints are formulated regarding train operation regulations and passenger capacity. In peak hours, the doors of a train usually open and close many times at each station because of excessive passenger flow, especially at transfer stations, resulting in delays to this and subsequent trains. The delayed train further increases the number of passengers gathered on the platform, putting additional pressure on the crew and causing potential safety hazards. Herein, the train dwell time is related to the number of passengers boarding and alighting the train at a station. The constraint on the train dwell time $t_{k,i}^{w}$ is as follows:

$$t_{k,i}^{w} = \beta\left(n_{k,i}^{al} + n_{k,i}^{b}\right) + d_i, \quad \forall k \in K;\ \forall i \in Z, \tag{5}$$

which indicates that the dwell time of train service k at station i is directly proportional to the total number of passengers boarding and alighting the train.

The train running time and interval constraints are as follows:

$$t_{k,i}^{d} = t_{k,i}^{a} + t_{k,i}^{w}, \quad \forall k \in K;\ \forall i \in Z, \tag{6}$$

$$t_{k,i+1}^{a} = t_{k,i}^{d} + t_{k,i}^{r}, \quad \forall k \in K;\ \forall i \in Z, \tag{7}$$

$$\begin{cases} t_{k,2I-1}^{r} = t_{\text{turnback},1}, & \forall k \in K, \\ t_{k,F}^{r} = t_{\text{turnback},F}, & \forall k \in K, \\ t_{k,I}^{r} = t_{\text{turnback},I}, & \forall k \in K, \end{cases} \tag{8}$$

$$t_{i,\min}^{r} \le t_{k,i}^{r} \le t_{i,\max}^{r} \quad \forall k \in K;\ \forall i \in Z, \tag{9}$$

$$h_{i,\min} \le h_{k,i} \le h_{i,\max}, \quad \forall k \in K;\ \forall i \in Z, \tag{10}$$

$$h_{k,i} = t_{k+1,i}^{d} - t_{k,i}^{d}, \quad \forall k \in K;\ \forall i \in Z, \tag{11}$$

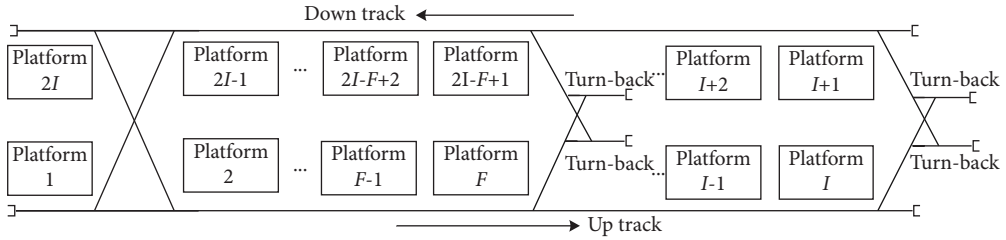

Figure 1: Schematic of the track layout of a URT line.

Table 1: Parameters and intermediate variables.

Notation	Definition
K	Set of train services
Z	Set of stations
T	Set of operation periods
k	Index of train services
i, r, j	Index of stations
$\delta_{k,i}$	Train load factor between stations i and $i+1$ for train service k
$t^w_{k,i}$	Dwell time at station i for train service k
β	Dwell-time coefficient
$n^{al}_{k,i}$	Number of passengers that alight train service k at station i
$n^{b}_{k,i}$	Number of passengers that board train service k at station i
d_i	Minimal dwell time at station i
$t^d_{k,i}$	Departure time of train service k at station i
$t^a_{k,i}$	Arrival time of train service k at station i
$t^r_{i,\min}$	Minimal running time from station i to station $i+1$
$t^r_{i,\max}$	Maximal running time from station i to station $i+1$
$h_{i,\min}$	Minimal train departure interval at station i
$h_{i,\max}$	Maximal train departure interval at station i
$t_{k,r1}$	Train running time of full-length routing
$t_{r1,\min}$	Minimal train running time of full-length routing
$t_{r1,\max}$	Maximal train running time of full-length routing
$t_{k,r2}$	Train running time of short-turn routing
$t_{r2,\min}$	Minimal train running time of short-turn routing
$t_{r2,\max}$	Maximal train running time of short-turn routing
t_{r1}	Average train running time of full-length routing
t_{r2}	Average train running time of short-turn routing
N_{r1}	Number of trains for full-length routing
N_{r2}	Number of trains for short-turn routing
N	Number of trains available
η	Train operation proportion of full-length and short-turn routings
h_{r1}	Average train departure interval of full-length routing
h_{r2}	Average train departure interval of short-turn routing
$l_k(t^d_{k,i})$	Number of passengers onboard train service k at station i after the boarding process has completed
$l_k(t^a_{k,i})$	Number of passengers onboard train service k at station i before the start of the boarding process
$n^b_{k,i,j}$	Number of passengers onboard train service k at station i with destination station j
$n^{t_1,t_2}_{i,j}$	Number of passengers arriving at station i with destination station j during time period $[t_1, t_2]$
$t^c_{k,i}$	Arrival time at station i of last passenger to board train service k
$l_{k,i}(t)$	Number of passengers onboard train service k at time t
δ_m	Maximum allowable train loading factor
c_k	Capacity of trains in terms of maximum number of onboard passengers
n^{t_1,t_2}_i	Number of passengers arriving at station i during time period $[t_1, t_2]$
$\tau_{i,j}(t)$	Passenger arrival rate at station i with destination station j at time t
$n^p_i(t^d_{k,i})$	Number of passengers waiting at station i after the boarding process has completed for train service k at station i
$n^p_{i,j}(t^d_{k,i})$	Number of passengers waiting at station i with destination station j after the boarding process has completed for train service k at station i
$t_{\text{turnback},i}$	Train turn-back time at reversal station
$\delta_{\max}$	Maximum loading rate of all the trains passing through each station
$t^r_{k,i}$	Running time from station i to station $i+1$ for train service k

Table 2: Decision variables.

Notation	Definition
$h_{k,i}$	Train departure interval at station i between train services k and $k+1$
$t_{k,i}^{r}$	Running time of train service k from station i to station $i+1$

$$t_{k,r1} = \sum_{i=1}^{2I-1} \left(t_{k,i}^{r} + t_{k,i}^{w}\right), \quad \forall k \in K, \tag{12}$$

$$t_{r1,\min} \le t_{k,r1} \le t_{r1,\max}, \quad \forall k \in K, \tag{13}$$

$$t_{k,r2} = \sum_{i=1}^{F} \left(t_{k,i}^{r} + t_{k,i}^{w}\right) + \sum_{i=2I-F+1}^{2I-1} \left(t_{k,i}^{r} + t_{k,i}^{w}\right), \quad \forall k \in K, \tag{14}$$

$$t_{r2,\min} \le t_{k,r2} \le t_{r2,\max}, \quad \forall k \in K. \tag{15}$$

Equation (6) indicates that the time at which train service k leaves station i is the time at which train service k arrives at station i plus the dwell time at station i. Equation (7) indicates that the time at which train service k arrives at station $i+1$ is the time at which train service k leaves station i plus its running time in section $[i, i+1]$. Equation (8) defines the turn-back time as the train's running time between the turn-back station and the reversal track. Equation (9) is the train's running time constraint between stations, and Equation (10) is the train departure interval constraint. The departure interval of adjacent trains at the same station must be greater than the minimum train departure interval of the station and less than the maximum train departure interval of the station. Equation (11) is the formula for calculating the departure interval of adjacent trains at station i. Equations (12)–(15) are the running-time constraints of full-length and short-turn routings.

In the following, equation (16) is the constraint for the number of trains required, and equations (17)–(19) are constraints on the average train departure interval for full-length and short-turn routings:

$$N_{r1} + N_{r2} \le N, \tag{16}$$

$$h_{r1} = \frac{t_{r1}}{N_{r1}}, \tag{17}$$

$$h_{r2} = \frac{t_{r2}}{N_{r2}}, \tag{18}$$

$$\frac{h_{r2}}{h_{r1}} = \eta. \tag{19}$$

The constraints in equations (20)–(28) are related to the train loading rate and passenger capacity, and when passenger demand exceeds the maximum loading capacity of the train, passengers will be unable to board the arriving train and will have to wait for subsequent trains:

$$l_k\left(t_{k,i}^{d}\right) = l_k\left(t_{k,i}^{a}\right) - n_{k,i}^{al} + n_{k,i}^{b}, \quad \forall k \in K;\ \forall i \in Z, \tag{20}$$

$$n_{k,i}^{b} = \sum_{j=i+1}^{2I} n_{k,i,j}^{b} = \sum_{j=i+1}^{2I} n_{i,j}^{t_{k-1,i}^{c}, t_{k,i}^{c}}, \quad \forall k \in K;\ \forall i \in Z, \tag{21}$$

$$t_{k,i}^{c} = \min\left\{t_{k,i}^{d}, \max\left\{t \middle| l_{k,i}(t) < \delta_{\max} c_k \le l_{k,i}(t) + n_i^{t,t+1}\right\}\right\}, \quad \forall k \in K;\ \forall i \in Z;\ \forall t \in T, \tag{22}$$

$$n_i^{t,t+1} = \sum_{j=i+1}^{2I} n_{i,j}^{t,t+1}, \quad \forall i \in Z;\ \forall t \in T, \tag{23}$$

$$n_i^{t_1,t_2} = \sum_{j=i+1}^{2I} n_{i,j}^{t_1,t_2} = \sum_{j=i+1}^{2I} \int_{t_1}^{t_2} \tau_{i,j}(t)\mathrm{d}t, \quad \forall i \in Z;\ \forall t_1, t_2 \in T, \tag{24}$$

$$n_{k,i}^{al} = \sum_{r=1}^{i-1} n_{k,r,i}^{b}, \quad \forall k \in K;\ \forall i \in Z, \tag{25}$$

$$n_i^{p}\left(t_{k,i}^{d}\right) = n_i^{p}\left(t_{k-1,i}^{d}\right) + n_i^{t_{k-1,i}^{d}, t_{k,i}^{d}} - n_{k,i}^{b} = \sum_{j=i+1}^{2I} \left[n_{i,j}^{p}\left(t_{k-1,i}^{d}\right) + n_{i,j}^{t_{k-1,i}^{d}, t_{k,i}^{d}} - n_{k,i,j}^{b}\right], \quad \forall k \in K;\ \forall i \in Z, \tag{26}$$

$$n_I^p\left(t_{k,I}^d\right) = n_F^p\left(t_{k,F}^d\right) = 0, \quad \forall k \in K, \tag{27}$$

$$\delta_{k,i} = \frac{l_k\left(t_{k,i}^d\right)}{c_k \le \delta_m}, \quad \forall k \in K;\ \forall i \in Z. \tag{28}$$

Equation (20) indicates that the number of passengers onboard train service k at station i after the boarding process has been completed is related to the number of passengers onboard train service k when it arrives at station i and the number of passengers boarding and alighting at station i. Equation (21) is the formula for the number of passengers boarding train service k at station i. Equations (22) and (23) show that, under the condition of passenger flow saturation, only some of the passengers on the platform can board the train because of the limited train capacity; the other passengers have to wait for the next train, where $t_{k,i}^c$ is the arrival time at station i of the last passenger to board train service k, $t_{k,i}^c \in (t_{k-1,i}^c, t_{k,i}^d)$. Equation (24) indicates that the number of passengers arriving at station i is the total number of passengers starting off at station i within the corresponding time range. Equation (25) specifies that the number of passengers alighting train service k at station i comprises the number of passengers boarding at all stations prior to station i with station i as the destination. Equation (26) indicates that the number of passengers waiting at station i after the boarding process has been completed for train service k at station i is related to the number of passengers waiting at station i when the previous train left station i, the number of passengers arriving at station i before train service k departs station i, and the number of passengers boarding at station i. Equation (27) specifies that all passengers alight at turn-back platforms I and F, and no passengers board the train. Equation (28) is the constraint for the maximum loading rate of the train.

3. Solution Approach

In essence, this problem is a large-scale combinatorial optimization problem. Simulated-annealing algorithms are effective for solving such problems, offering satisfactory solutions in a reasonable time. Herein, a heuristic simulated-annealing algorithm is designed to solve the model.

3.1. Simulated-Annealing Algorithm. The current regular schedule is used as the initial solution. The O-D time-varying passenger flow is distributed to each scheduled train service, and the simulated-annealing algorithm is iterated to approach the minimum value of the objective function. Figure 2 shows a flowchart of the simulated-annealing algorithm. The solution steps are as follows:

Step 1. We initialize the algorithm parameters, including the initial temperature t_s, termination temperature t_e, temperature attenuation coefficient a, Markov chain length m_l, current iteration number Ite, total number of individuals M, and current solved individual m.

Step 2. We take the current regular train operation scheme s_0 as the initial train operation scheme and calculate the initial objective function value as $f(s_0)$. The current global optimal objective function value is $f(s_{\min}) = f(s_0)$, and the individual optimal objective function value is $f(s) = f(s_0)$.

Step 3. For individual m and the corresponding operation plan, a new operation plan s_{new} is generated using the multineighborhood moving criterion, and the objective function value is $f(s_{\text{new}})$.

Step 4. If $f(s_{\text{new}}) > f(s)$, we accept the neighborhood solution S_{new} according to the Metropolis criterion; if $f(s_{\text{new}}) \le f(s)$, we record the neighborhood solution S_{new} as the optimal solution for individual m.

Step 5. If all individuals have been traversed, we select the optimal solution from the M individuals and record it as the global optimal objective value $f(s_{\min})$, then set $m = 1$; otherwise, we return to step 3 and set $m = m + 1$.

Step 6. We set $t = at$. If $t < t_e$, we terminate the algorithm; otherwise, we return to step 3.

3.2. Adaptive Large Neighborhood Search Metaheuristic. An adaptive large neighborhood search (ALNS) metaheuristic is now proposed to search neighboring solutions efficiently and reasonably. The operators are chosen via the roulette-wheel mechanism at each iteration, with a probability that depends on their former performance. For a detailed formulation, see equation (29), in which p_i represents the probability of operator i being selected, κ_i represents the weight of operator i and has an initial value of 1, and N_d represents the total number of operators that can be selected.

$$p_i = \frac{\kappa_i}{\sum_{j=1}^{N_d} \kappa_j}, \quad \forall i, j \le N. \tag{29}$$

Each search process is divided into segments of ψ iterations. Each operator i is assigned a score π_i, with the initial score set to 0. After each iteration, the score of the selected operator increases by c_1 if a new best solution is found, increases by c_2 if a solution better than the previous one but worse than the best one is found, and increases by c_3 if the solution is worse than the previous one but still accepted via the simulated-annealing acceptance criterion. At the end of each segment, the weights of the selected operators are calculated by considering the scores obtained in the last ψ iterations according to

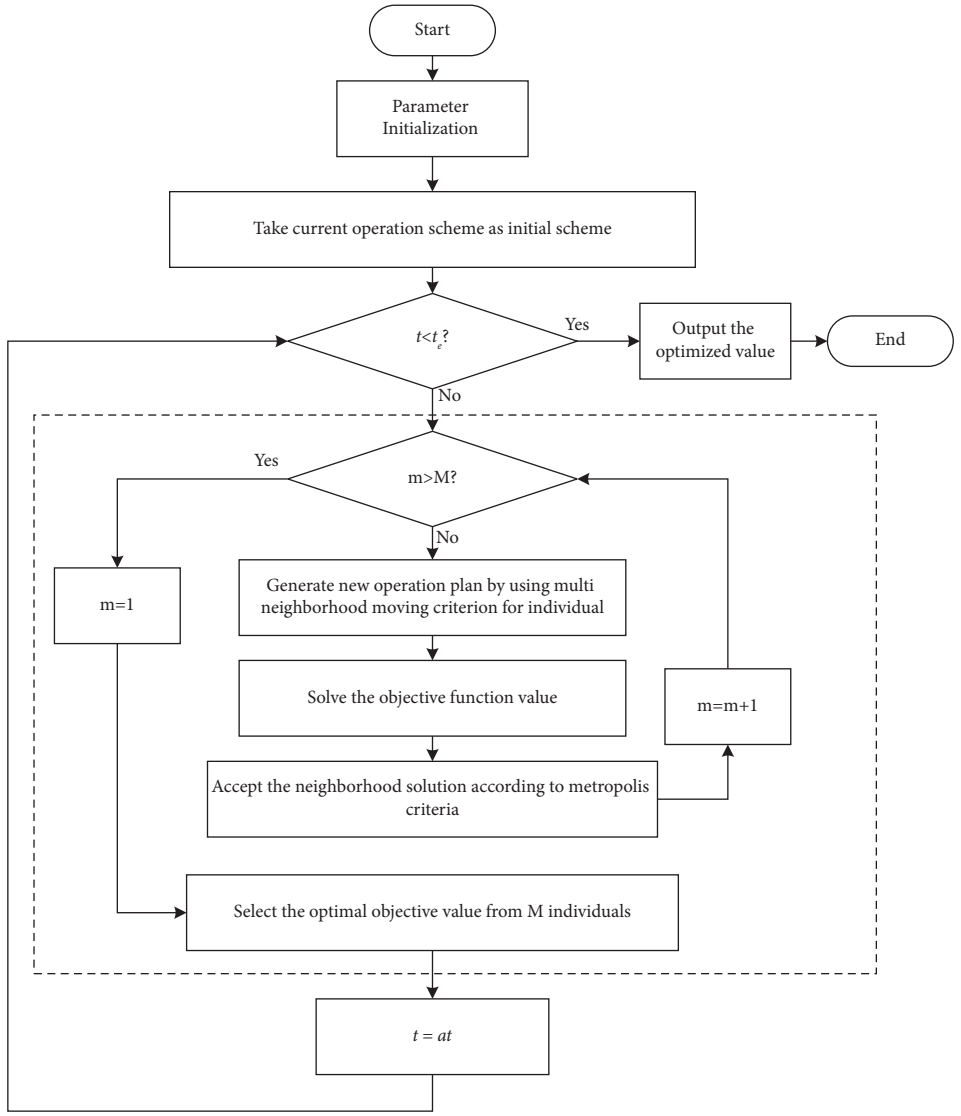

Figure 2: Flowchart of the parallel-simulated-annealing algorithm.

$$\kappa_i = \begin{cases} \kappa_i, & \text{if } n_{ij} = 0, \\ (1-\omega)\kappa_i + \dfrac{\omega\pi_i}{n_{ij}}, & \text{if } n_{ij} \neq 0, \end{cases} \tag{30}$$

where ω represents the weight reaction index, which controls the effect of past performance, and n_{ij} represents the number of times operator i has been used in segment j. At the end of each segment, the scores of all operators are reset to 0. In the proposed implementation, the length of segment ψ is set to 100, the weight reaction index ω is set to 0.8, and c_1, c_2, and c_3 are set to 10, 6, and 3, respectively.

As the train headway $h_{k,i}$ and train running time between stations $t^r_{k,i}$ are decision variables in the proposed model, their output datasets $O(h_{k,i})$ and $O(t^r_{k,i})$ constitute the solution of the model. The expressions of $O(h_{k,i})$ and $O(t^r_{k,i})$ are of the form

$$O\left(h_{k,i}\right) = \begin{pmatrix} h_{1,1} & h_{1,2} & h_{1,3} & \cdots & h_{1,2I-1} \\ h_{2,1} & h_{2,2} & h_{2,3} & \cdots & h_{2,2I-1} \\ \vdots & \vdots & \vdots & \ddots & \vdots \\ h_{k-1,1} & h_{k-1,2} & h_{k-1,3} & \cdots & h_{k-1,2I-1} \end{pmatrix},$$
$$O\left(t^{\mathrm{r}}_{k,i}\right) = \begin{pmatrix} t^{\mathrm{r}}_{1,1} & t^{\mathrm{r}}_{1,2} & t^{\mathrm{r}}_{1,3} & \cdots & t^{\mathrm{r}}_{1,2I-1} \\ t^{\mathrm{r}}_{2,1} & t^{\mathrm{r}}_{2,2} & t^{\mathrm{r}}_{2,3} & \cdots & t^{\mathrm{r}}_{2,2I-1} \\ \vdots & \vdots & \vdots & \ddots & \vdots \\ t^{\mathrm{r}}_{k,1} & t^{\mathrm{r}}_{k,2} & t^{\mathrm{r}}_{k,3} & \cdots & t^{\mathrm{r}}_{k,2I-1} \end{pmatrix}. \tag{31}$$

As shown in equation (32), the operators $\Delta h_{k,i}$ and $\Delta t^r_{k,i}$ denote the offsets of train headway and running time, respectively. The values of these operators should be small enough to guarantee that the generated neighbors are feasible solutions. Thus, each $\Delta h_{k,i}$ and $\Delta t^r_{k,i}$ are randomly defined as −1, 0, or 1; $O(\Delta h_{k,i})$ and $O(\Delta t^r_{k,i})$ are datasets of $\Delta h_{k,i}$ and $\Delta t^r_{k,i}$, respectively.

$$O\left(\Delta h_{k,i}\right)=\begin{pmatrix}\Delta h_{1,1} & \Delta h_{1,2} & \Delta h_{1,3} & \ldots & \Delta h_{1,2\mathrm{I}-1}\\ \Delta h_{2,1} & \Delta h_{2,2} & \Delta h_{2,3} & \ldots & \Delta h_{2,2\mathrm{I}-1}\\ \vdots & \vdots & \vdots & \ddots & \vdots\\ \Delta h_{k-1,1} & \Delta h_{k-1,2} & \Delta h_{k-1,3} & \ldots & \Delta h_{k-1,2\mathrm{I}-1}\end{pmatrix},$$

$$O\left(\Delta t^{\mathrm{r}}_{k,i}\right)=\begin{pmatrix}\Delta t^{\mathrm{r}}_{1,1} & \Delta t^{\mathrm{r}}_{1,2} & \Delta t^{\mathrm{r}}_{1,3} & \ldots & \Delta t^{\mathrm{r}}_{1,2\mathrm{I}-1}\\ \Delta t^{\mathrm{r}}_{2,1} & \Delta t^{\mathrm{r}}_{2,2} & \Delta t^{\mathrm{r}}_{2,3} & \ldots & \Delta t^{\mathrm{r}}_{2,2\mathrm{I}-1}\\ \vdots & \vdots & \vdots & \ddots & \vdots\\ \Delta t^{\mathrm{r}}_{k,1} & \Delta t^{\mathrm{r}}_{k,2} & \Delta t^{\mathrm{r}}_{k,3} & \ldots & \Delta t^{\mathrm{r}}_{k,2\mathrm{I}-1}\end{pmatrix}. \tag{32}$$

A new neighbor s_{new} is generated via equation (33). If the generated neighbor is not a feasible solution, it is ignored, and a new neighbor is generated according to the previously mentioned rules.

$$\begin{cases} O\left(h_{k,i}\right)_{\mathrm{new}}=O\left(h_{k,i}\right)+O\left(\Delta h_{k,i}\right),\\ O\left(t^{r}_{k,i}\right)_{\mathrm{new}}=O\left(t^{r}_{k,i}\right)+O\left(\Delta t^{r}_{k,i}\right),\end{cases} \tag{33}$$

3.3. Solution Procedure. The detailed procedure of the simulated-annealing algorithm with the ALNS metaheuristic is as follows:

(1) Initialize: we generate a regular schedule and take it as initial solution s_0 with object function value $f(s_0)$.

(2) For each operator, we set weight = 1 and score = 0.

(3) $s_{\min}\leftarrow s\leftarrow s_0, t\leftarrow t_s$.

(4) We initialize the number of individuals $1\leftarrow m$.

(5) We initialize the number of iterations $1\leftarrow Ite$.

(6) We select operators $O(\Delta h_{k,i})$ and $O(\Delta t^{r}_{k,i})$ via the roulette-wheel mechanism at each iteration based on their current weights and apply the operators to solution s to generate a neighbor solution s_{new} according to equation (33).

(7) We check the feasibility of neighbor solution s_{new} according to equations (5)–(28). If the neighbor solution is not feasible, we ignore it and return to step 6 to generate a new neighbor.

(8) We calculate the object value $f(s_{\mathrm{new}})$ for neighbor solution s_{new}.

(9) If $f(s_{\mathrm{new}})\le f(s)\le f(s_{\min})$, we go to step 10; otherwise, go to step 11.

(10) $s_{\min}\leftarrow s\leftarrow s_{\mathrm{new}}$, we update the score for the selected operator with c_1.

(11) If $f(s_{\min})\le f(s_{\mathrm{new}})\le f(s)$, we go to step 12; otherwise, go to step 13.

(12) $s\leftarrow s_{\mathrm{new}}$, we update the score for the selected operator with c_2.

(13) If $f(s_{\mathrm{new}})>f(s)$ but s_{new} is accepted by the simulated-annealing criterion, we go to step 14.

(14) $s\leftarrow s_{\mathrm{new}}$, we update the score for the selected operator with c_3.

(15) $Ite = Ite + 1$, $m = m + 1$.

(16) If $Ite\le\psi$, go to step 6.

(17) If Ite has reached the defined length of segment ψ ($Ite>\psi$), we go to step 18.

(18) We update the weights for all involved operators according to equation (30), reset score = 0 for all operators.

(19) If $m\le M$, we go to step 5.

(20) If $m>M$, we go to step 21.

(21) $t\leftarrow at$.

(22) If $(t\ge t_e)$, we go to step 4.

(23) If $(t<t_e)$, we go to step 24.

(24) We return $s_{\min}$ and the corresponding object function value, end.

4. Case Study

We consider a URT line of length 45.34 km with 25 stations. In total, 50 platforms are set for the up and down directions, and platform 19 is a turn-back platform for short-turn routing. All trains are six-car marshaling type-B trains. The trains turn back before the initial station and after the tail station. Figure 3 shows the passenger numbers during peak hours. Because the passenger flow on each section of the line is unbalanced, long-length and short-turn routings with a 2 : 1 train operation proportion ($\eta=2$) are used.

The proposed algorithm was programmed in MATLAB R2019b on a personal computer with an Intel® Core™ i3–9100 3.60 GHz CPU with 8.00 GB of memory and the Windows 10 64-bit operating system. The current regular train operation plan was used as the initial solution, with a train operation proportion of 2 : 1 for full-length and short-turn routings ($\eta=2$). The weight coefficient of the objective function was set to $\lambda=0.5$. The average train departure interval of adjacent trains h_{ave} was set to 120–170 s, i.e., a fixed value for h_{ave} is taken in equation (3) as a constraint. For each given average train departure interval h_{ave}, the initial temperature t_s was set to 500, the termination temperature t_e was set to 1, the temperature attenuation coefficient a was set to 0.85, and the Markov chain length m_l was set to 1000.

4.1. Results and Discussion. The simulated-annealing algorithm process terminated after running for 546 s, and the algorithm converged rapidly and tended to stabilize for the optimal solution after 3800 iterations. This indicates that the convergence behavior of the algorithm is good.

The minimum value of the objective function min f = 4.02 with an average train departure interval of $h_{\mathrm{ave}}=120$ s gives a maximum train loading rate of $\delta_{\max}=0.844$ and an average deviation of $h_{\Delta}=3.82$ s in the train departure interval. Table 3 presents a detailed comparison of the optimized irregular schedule and the regular schedule.

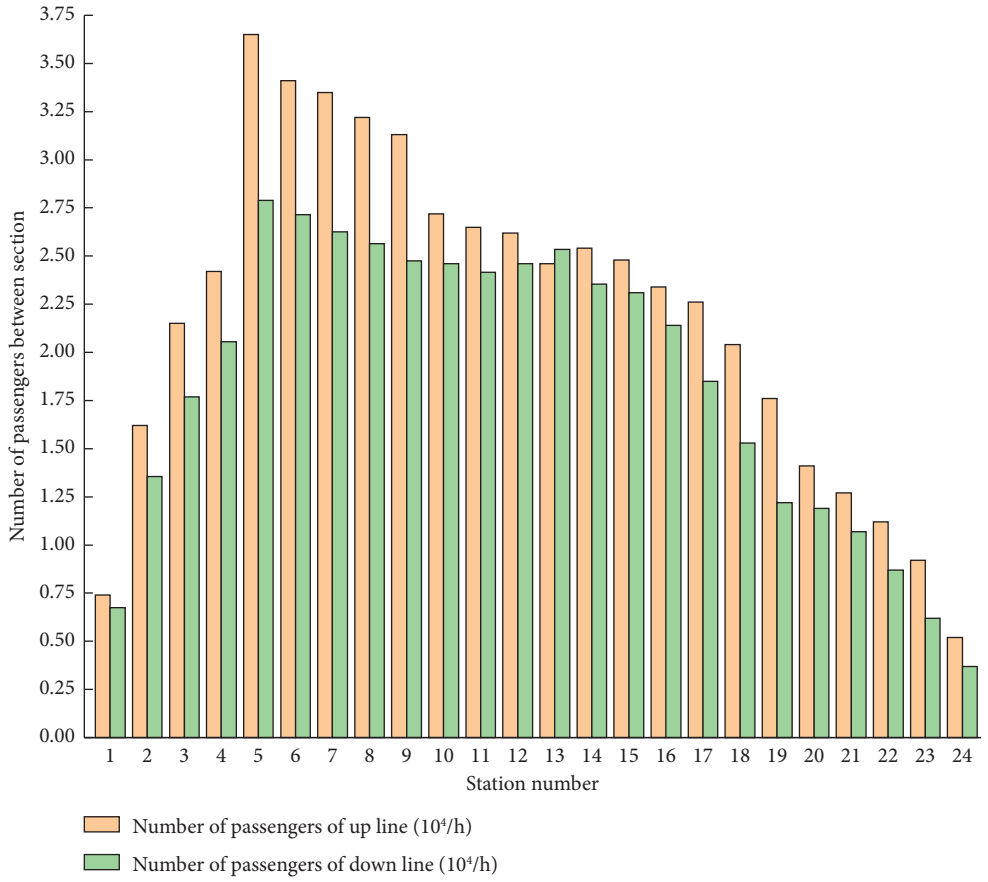

Figure 3: Number of passengers during peak hours.

Table 3: Comparison of values under an optimized irregular schedule and the current regular schedule.

Station index	Length (m)	DT1 (s)	DT2 (s)	Gap1 (%)	LR1	LR2	Gap3 (%)
1	657	40	38	−5.0	0.173	0.171	−1.2
2	1361	30	28	−6.7	0.380	0.375	−1.3
3	857	35	32	−8.6	0.506	0.498	−1.6
4	1425	35	34	−2.9	0.578	0.561	−2.9
5	1602	55	58	+5.5	0.872	0.844	−3.2
6	1744	30	29	−3.3	0.818	0.789	−3.5
7	1146	50	48	−4.0	0.802	0.775	−3.4
8	1074	30	26	−13.3	0.774	0.746	−3.6
9	1303	35	33	−5.7	0.749	0.725	−3.2
10	1587	45	42	−6.7	0.647	0.629	−2.8
11	1183	30	29	−3.3	0.632	0.613	−3.0
12	1085	30	28	−6.7	0.625	0.606	−3.0
13	874	30	30	0	0.588	0.569	−3.2
14	1199	45	41	−8.9	0.605	0.587	−3.0
15	860	30	29	−3.3	0.593	0.574	−3.2
16	1023	30	28	−6.7	0.560	0.541	−3.4
17	1435	40	37	−7.5	0.541	0.523	−3.3
18	1908	30	27	−10.0	0.487	0.472	−3.1
19	6924	50	46	−8.0	0.629	0.611	−2.9
20	1784	35	33	−5.7	0.507	0.489	−3.6
21	3361	25	23	−8.0	0.455	0.440	−3.3
22	1894	30	29	−3.3	0.401	0.389	−3.0
23	1540	40	35	−12.5	0.329	0.319	−3.0
24	5895	30	28	−6.7	0.186	0.181	−2.7
25	437	40	37	−7.5	—	—	—
SUM	44158	900	848	−5.8	—	—	—

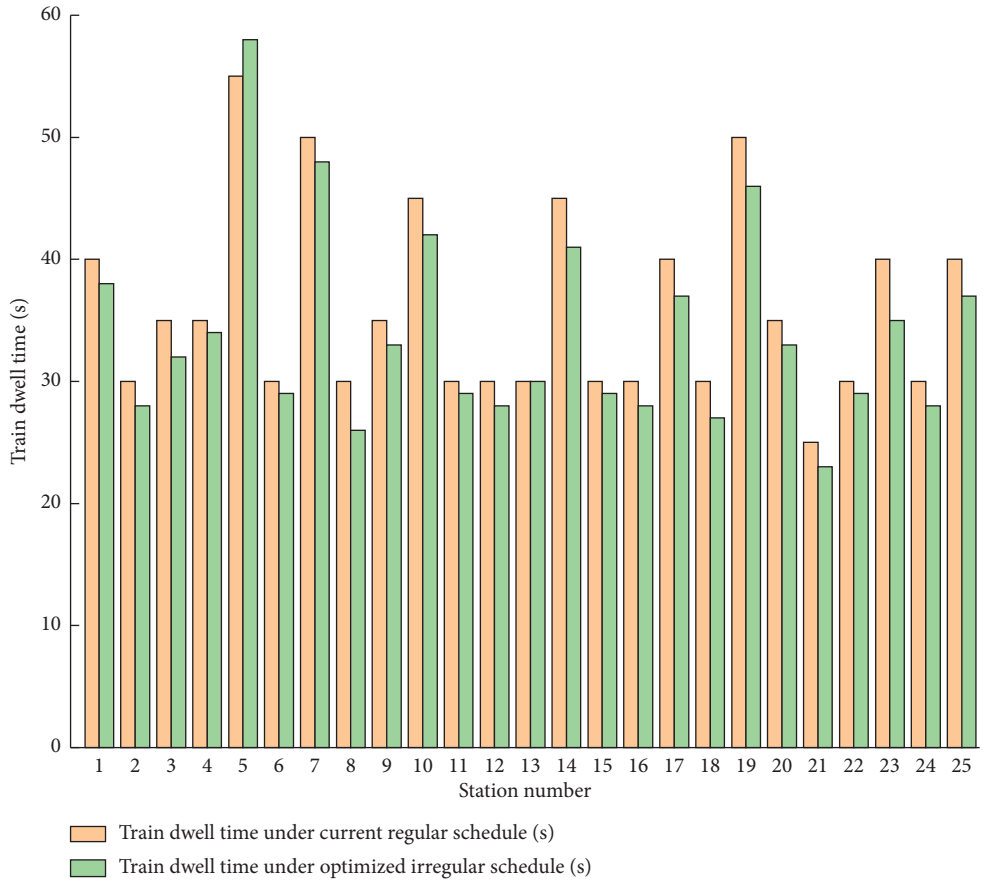

Figure 4: Train dwell times under optimized irregular schedule and current regular schedule.

In Table 3, DT1 refers to the train dwell time at different stations under the regular train schedule, while DT2 refers to that under the optimized irregular train schedule. As indicated in equation (5), the train dwell time under the optimization model is related to the number of passengers boarding and alighting this train at the station. Figure 4 shows that the up-track train dwell time under the optimized irregular schedule is lower than that under the regular schedule at most stations, although the dwell time at station 5 has increased. The reason for this increase is that station 5 is a transfer station and has the largest passenger flow over the whole line (as shown in Figure 3). The current dwell time of 55 s does not meet the passengers' needs for boarding and alighting, whereas the optimized dwell time of 58 s accurately matches passenger demand. Table 3 indicates that the total train dwell time from station 1 to station 25 decreases from 900 s to 848 s under the optimized irregular schedule, thus reducing passenger travel times and improving operational efficiency.

We now investigate the average waiting time and average travel time of passengers under the optimized schedule. The average waiting time $T_{\text{ave\_wait}}$ and average travel time $T_{\text{ave\_tra}}$ are calculated according to equations (34) and (35), respectively, where T_{wait} is the total waiting time of all passengers, $T_{\text{tra\_train}}$ is the total travel time of passengers within the train, and N_p is the total number of passengers. As shown in equation (36), the total waiting time of passengers T_{wait} consists of the waiting time of passengers boarding the current train and the waiting time of passengers who remain on the platform. $T_{\text{tra\_train}}$ and N_p are calculated according to equations (37) and (38), respectively.

$$T_{\text{ave\_wait}} = \frac{T_{\text{wait}}}{N_p}, \tag{34}$$

$$T_{\text{ave\_tra}} = \frac{T_{\text{wait}} + T_{\text{tra\_train}}}{N_p}, \tag{35}$$

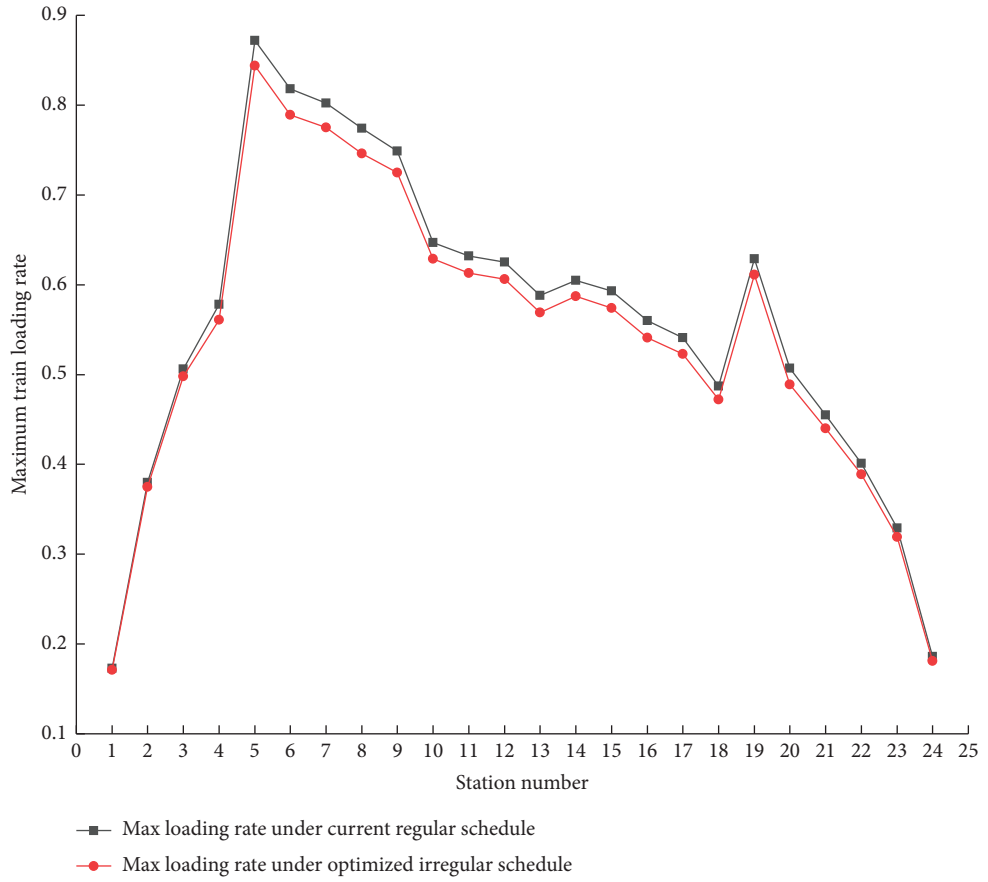

Figure 5: Maximum train loading rate under the optimized irregular schedule and current regular schedule.

$$T_{\text{wait}} = \sum_{k=1}^{K}\sum_{i=1}^{2I}\sum_{j>i}^{2I}\int_{t_{k-1,i}^{d}}^{t_{k,i}^{d}} \tau_{i,j}(t)\cdot\left(t_{k,i}^{d}-t\right)\mathrm{d}t + \sum_{k=1}^{K}\sum_{i=1}^{2I} n_i^{p}\left(t_{k,i}^{d}\right)\cdot\left(t_{k+1,i}^{d}-t_{k,i}^{d}\right), \tag{36}$$

$$T_{\text{tra\_train}} = \sum_{k=1}^{K}\sum_{i=1}^{2I-1} l_k\left(t_{k,i}^{d}\right)\cdot\left(t_{k,i+1}^{a}-t_{k,i}^{d}\right), \tag{37}$$

$$N_p = \sum_{k=1}^{K}\sum_{i=1}^{2I}\sum_{j>i}^{2I}\int_{t_{k-1,i}^{d}}^{t_{k,i}^{d}} \tau_{i,j}(t)\mathrm{d}t. \tag{38}$$

The reductions in train dwell time and running time between stations mean that the average waiting time of passengers after optimization is 2.8 s less than that before optimization, an optimization ratio of 4.3%. The average travel time of passengers after optimization is reduced by 42 s, an optimization ratio of 5.7%, which shows that the optimization model established in this paper has a positive effect on improving travel efficiency.

In Table 3, LR1 refers to the maximum train loading rate at different stations under the regular schedule, while LR2 refers to that under the optimized irregular schedule. Figure 5 shows that, through accurate matching of the train timetable with the passenger flow under the optimized irregular schedule, the maximum train loading rate at each station has been reduced to varying degrees compared with the current regular schedule. Table 3 illustrates that the reduction ratio of the maximum train loading rate ranges from 1.2% to 3.6%.

According to Table 3, the maximum train loading rate is 0.844 at station 5 after optimization, with an optimization ratio of 3.2% compared with that before optimization. To clarify the root cause for this optimization, Figure 6 shows the train departure intervals under both the original and optimized schedules.

Forty-five trains are dispatched from station 5 under both the current regular schedule and the optimized irregular schedule in the peak hours between 07:00 and 08:30, with the same average departure interval of 120 s. As shown in Figure 6, the train departure interval under the current regular schedule is fixed at 120 s, whereas it ranges from 115

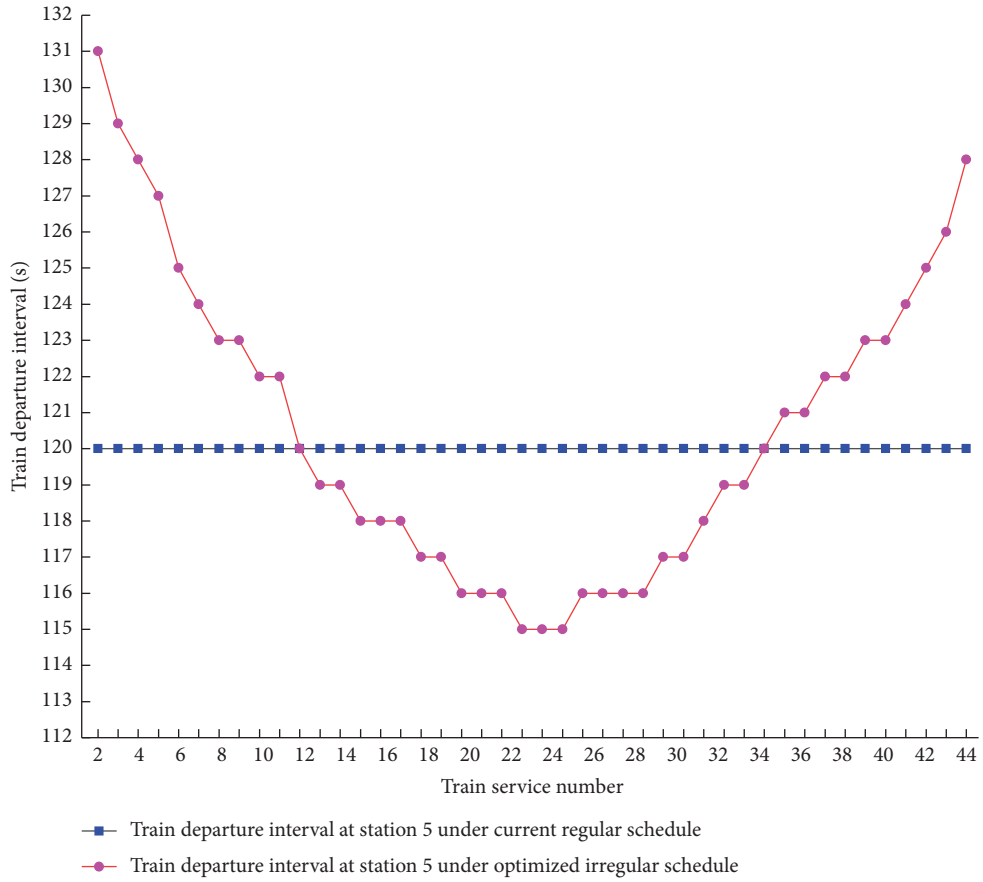

Figure 6: Train departure intervals under the optimized irregular schedule and current regular schedule.

to 131 s under the optimized irregular schedule. The optimized train headway is relatively dense in the middle of the peak period and relatively sparse in other periods. The optimized train departure intervals gradually decrease from 131 s to 120 s between 07:00:00 and 07:23:54 and remain below 120 s from 07:23:55 to 08:06:47, with minimum departure intervals of 115 s between 07:43:28 and 07:49:13. The optimized train departure intervals then increase from 120 s to 128 s between 08:06:48 and 08:30:00.

According to the passenger flow statistics, the passenger arrival rate at each station during peak hours does not obey a uniform or Poisson distribution. The passenger arrival at station 5 is concentrated between 07:25 and 08:05, reaching a maximum at 07:48. The passenger arrival rate increases gradually before this time and decreases gradually thereafter. The changes in the train departure interval and passenger arrival rate are clearly consistent with each other under the optimized irregular schedule. Thus, it can be concluded that the basic reason for the optimization of the maximum train loading rate is that the train departure intervals decrease during the period of maximum passenger arrival, but the total number of train services does not increase.

Figure 7 compares the optimized irregular schedule with the regular schedule under different average departure intervals h_{ave}. Under the same h_{ave}, the optimized irregular schedule reduces the maximum train loading rate significantly. Compared with the regular schedule, the maximum train loading rate of the collinear and noncollinear sections decreases by 3.21%–4.82% and 2.52%–3.64%, respectively, when h_{ave} is set as 120–170 s. The optimization range of the maximum train loading rate of the collinear section is slightly higher than that of the noncollinear section. This is because the passenger flow of the collinear section is higher than that of the noncollinear section, while the optimization objective is the maximum train loading rate of each section.

At present, train schedule no. 92 is used for daily operation, with a regular interval of 170 s, a maximum train loading rate of $\delta_{max} = 123.8\%$, and an average train loading rate of $\delta_{ave} = 82.3\%$. The optimized irregular train schedule gives the lowest train loading rate when the average departure interval h_{ave} is set to 120 s; in this case, the maximum train loading rate δ_{max} is 84.4% and the average train loading rate δ_{ave} is 53.7%, reduction ratios of 31.8% and 34.8%, respectively, compared with regular train schedule no. 92.

4.2. Sensitivity Analysis

4.2.1. Impact of Nonnegative Weight Coefficient λ. Figures 8 and 9 show that as the coefficient weight λ increases from 0 to 1.0, the maximum train loading rate δ_{max} gradually decreases from 0.872 to 0.809, and the average deviation in the train departure interval h_{Δ} gradually

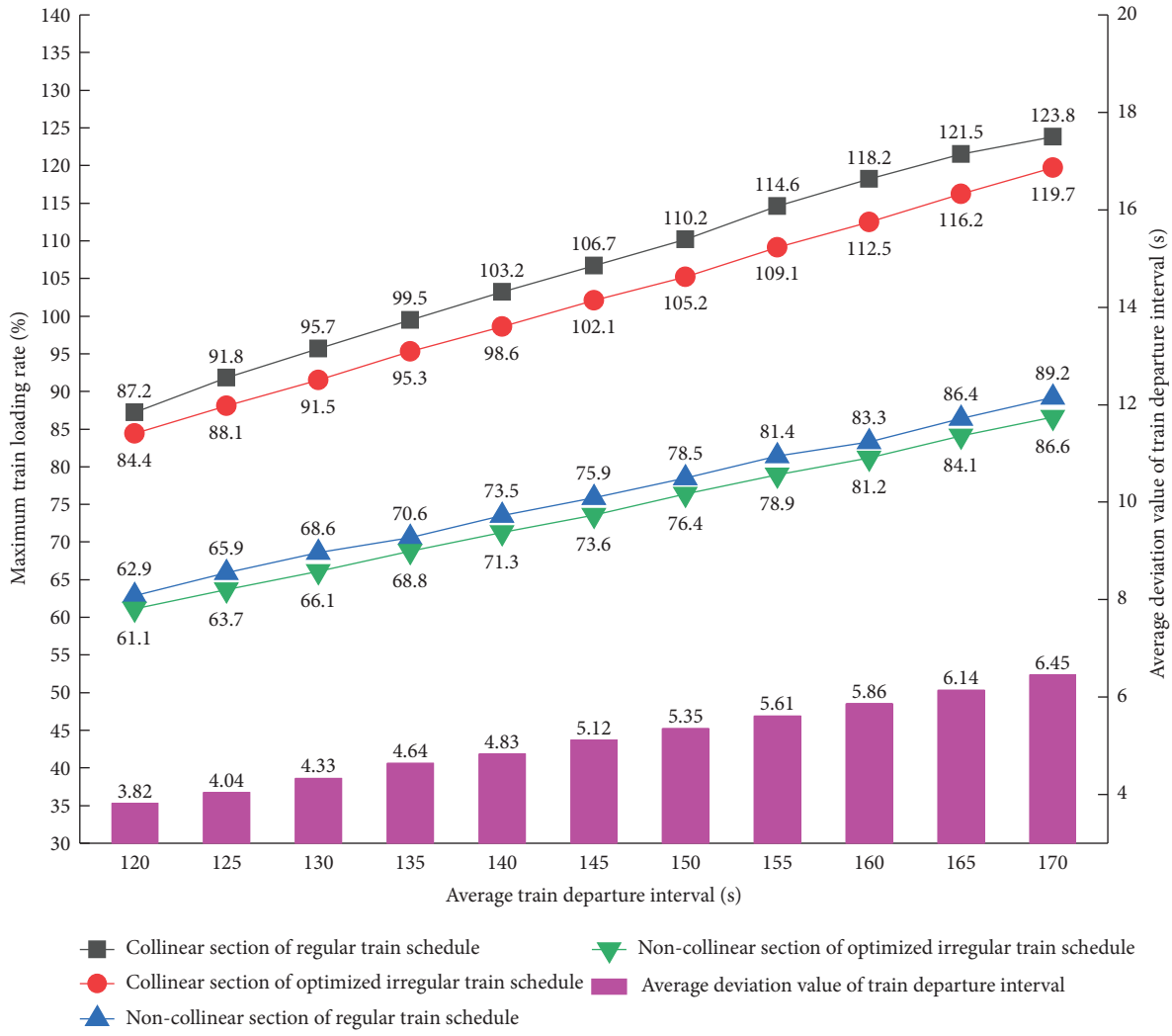

Figure 7: Comparison of results between an optimized irregular schedule and a regular schedule.

increases from 0 s to 5.173 s. This is obviously consistent with the actual situation. In particular, when $\lambda = 0$, we have $\min f = 5\lambda\delta_{\max} + (1-\lambda)h_{\Delta} = 0$, in which case the optimized train schedule corresponds to the regular-interval schedule with a maximum loading rate of $\delta_{\max} = 0.872$.

4.2.2. Impact of the Average Train Departure Interval h_{ave}. As shown in Figure 7, under the optimized irregular schedule, a smaller average train departure interval h_{ave} produces a smaller maximum train loading rate $\delta_{\max}$ and average deviation in the train departure interval h_{Δ}. Therefore, compressing the train departure interval is an important means of improving passenger comfort.

Table 4 and Figure 7 show that when the average train departure interval h_{ave} is reduced from 170 s to 120 s, the maximum train loading rate of the whole line $\delta_{\max}$ decreases from 119.7% to 84.4%, that of the noncollinear section $\delta_{\max\_non-co}$ decreases from 86.6% to 61.1%, and the average deviation of the train departure interval h_{Δ} decreases from 6.45 s to 3.82 s. Table 4 also illustrates that a shorter average train departure interval h_{ave} gives a smaller average train loading rate and requires more trains. When h_{ave} is reduced from 170 s to 120 s, the average train loading rate of the whole line δ_{ave} decreases from 76.9% to 53.7%, that of the noncollinear section $\delta_{\text{ave\_non-co}}$ decreases from 57.4% to 40.5%, and the number of trains required N_{require} increases from 40 to 56. Equation (39) gives the average train loading rate of the whole line, and equation (40) gives that for the noncollinear section:

$$\delta_{\text{ave}} = \frac{\sum_{k=1}^{K}\sum_{i=1}^{2I}\delta_{k,i}}{K(2I-2)}, \tag{39}$$

$$\delta_{\text{ave\_non-co}} = \frac{\sum_{k=1}^{K}\sum_{i=F+1}^{2I-F}\delta_{k,i}}{K(2I-2F-1)}. \tag{40}$$

4.2.3. Impact of Train Operation Proportion of Full-Length and Short-Turn Routings η. As shown in Figure 10, the proportion of full-length and short-turn routings η has a significant impact on the required number of trains N_{require}

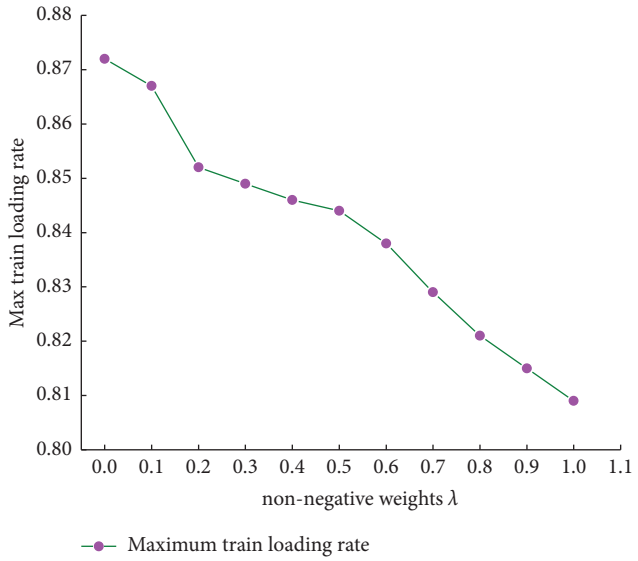

Figure 8: Maximum train loading rate under different weights λ.

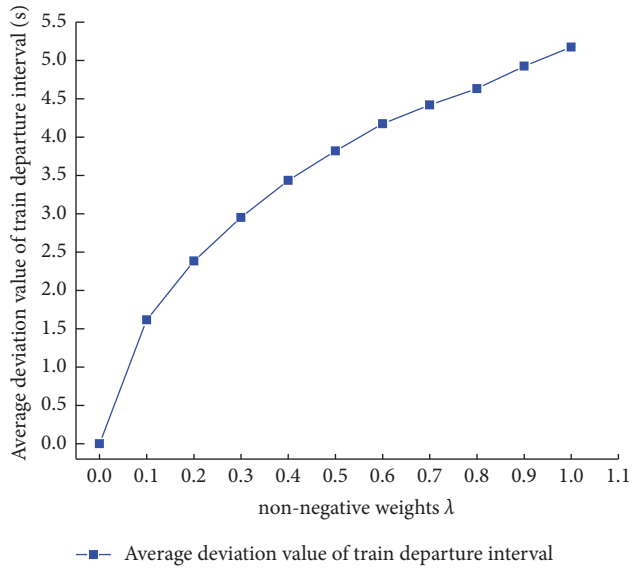

Figure 9: Average deviation in the train departure interval under different weights λ.

and the average train loading rate of the whole line δ_{ave}. A reduction in η reduces $N_{require}$ under the same average train departure interval but increases the average train loading rate δ_{ave}. Figure 10 shows that when the average train departure interval h_{ave} is 120 s and η is 2 : 1, $N_{require} = 56$ and $\delta_{ave} = 53.7\%$, whereas when η is 1 : 1, $N_{require}$ decreases to 53 and δ_{ave} increases to 57.7%.

Under an average train departure interval h_{ave} of 120 s, when the train operation proportion of full-length and short-turn routings η is reduced from 2 : 1 to 1 : 1, the average train loading rate at noncollinear sections δ_{ave_non-co} increases from 40.5% to 54.2%, and the maximum train loading rate at noncollinear sections δ_{max_non-co} increases from 61.1% to 81.5%. Therefore, compared with $\eta = 2:1$, $\eta = 1:1$ improves the equilibrium of the train loading rate between collinear and noncollinear sections. If η is reduced further (e.g., 1 : 2), the maximum train loading rate at noncollinear sections δ_{max_non-co} becomes too high and passenger comfort is affected, which is not recommended.

The previously mentioned sensitivity analysis results are consistent with expectations, which proves that the model in this paper has good usability and reliability, and can be applied to URT train schedule optimization.

Table 4: Optimization results with 2 : 1 train operation proportion of full-length and short-turn routings.

h_{ave} (s)	Number of trains $N_{require}$	Number of trains required		Max. loading rate (%)		Average loading rate (%)		h_{Δ} (s)
		Full-length routing N_{r1}	Short-turn routing N_{r2}	δ_{max}	δ_{max_non-co}	δ_{ave}	δ_{ave_non-co}	
170	40	30	10	119.7	86.6	76.9	57.4	6.45
165	41	31	10	116.2	84.1	74.6	55.6	6.14
160	42	32	10	112.5	81.2	72.2	54.2	5.86
155	44	33	11	109.1	78.9	70.1	52.3	5.61
150	45	34	11	105.2	76.4	67.9	50.4	5.35
145	47	35	12	102.1	73.6	65.2	48.9	5.12
140	48	36	12	98.6	71.3	63.2	47.3	4.83
135	50	38	12	95.3	68.8	60.1	45.6	4.64
130	52	39	13	91.5	66.1	57.8	43.8	4.33
125	54	41	13	88.1	63.7	55.2	42.1	4.04
120	56	42	14	84.4	61.1	53.7	40.5	3.82

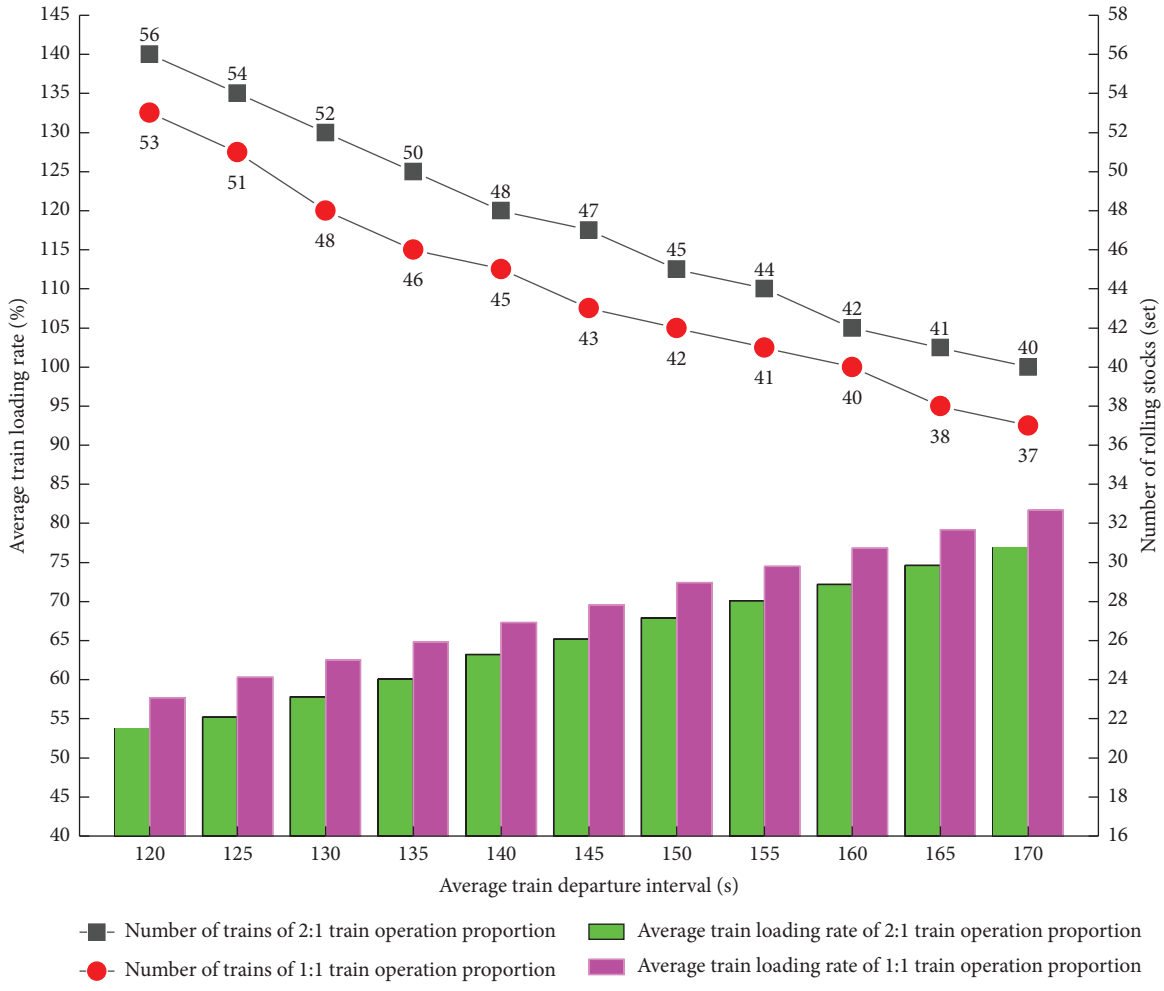

Figure 10: Optimization results for an irregular schedule with different train operation proportions.

5. Conclusions and Future Research

Taking the maximum train loading rate and average deviation in the departure interval as the cooperative optimization objectives, this paper has established an optimization model for an irregular train schedule that operates over peak hours to improve the passenger experience. A case study showed that, under the optimized irregular schedule, the train capacity can be better matched with the passenger flow. The minimum value of

the objective function is obtained with an average train departure interval of 120 s. The total train dwell time from stations 1–25 decreases from 900 s under the existing regular schedule to 848 s under the optimized irregular schedule, and the maximum train loading rate decreases by 1.2%–3.6% at the various stations. Compared with the regular schedule, the maximum train loading rate of the collinear and noncollinear sections decreases by 3.21%–4.82% and 2.52%–3.64%, respectively, when h_{ave} is set as 120–170 s.

Sensitivity analysis was considered for the nonnegative weight coefficient λ, average train departure interval h_{ave}, and proportion of full-length and short-turn routings η. Increasing λ from 0 to 1.0 produces a gradual decrease in δ_{max} from 0.872 to 0.809, while h_{Δ} gradually increases from 0 s to 5.173 s. When h_{ave} is reduced from 170 s to 120 s, the maximum train loading rate decreases from 119.7% to 84.4%, the average train loading rate decreases from 76.9% to 53.7%, and the average deviation in the train departure interval decreases from 6.45 s to 3.82 s. The proportion of full-length and short-turn routings η has a significant impact on the number of trains required and the equilibrium of the train loading rate. Reducing η from 2 : 1 to 1 : 1 reduces the number of trains required by three for $h_{ave} = 120$ s and improves the equilibrium of the train loading rate between collinear and noncollinear sections to make the capacity configuration more reasonable.

The research object in this study was train-scheduling optimization for URT. It was assumed that all trains enter the next service after completing their turn-back operation, without considering the situation of trains entering and leaving the depot. To consider train scheduling for the whole day, it will be necessary to consider the train connection plan and carry out collaborative optimization of the train schedule and turnover plan.

Data Availability

The data used to support the findings of this study are available from the corresponding author upon request.

Conflicts of Interest

The authors declare that they have no conflicts of interest.

Acknowledgments

This research was supported by the National Key R&D Program of China (grant nos. 2017YFB1200702 and 2016YFC0802208), the National Natural Science Foundation of China (grant nos. 52072314 and 52102391), the Sichuan Science and Technology Program (grant nos. 2020YFH0035, 2020YJ0268, 2020YJ0256, and 2020JDRC0032), the Science and Technology Plan of the China Railway Corporation (grant nos. P2018T001 and 2019KY10), and the Chengdu Science and Technology Plan Research Program (grant nos. 2019-YF05-01493-SN, 2020-RK00-00036-ZF, and 2020-RK00-00035-ZF).

References

[1] V. F. Hurdle, "Minimum cost schedules for a public transportation route-I. Theory," *Transportation Science*, vol. 7, no. 2, pp. 109–137, 1973.

[2] P. Serafini and W. Ukovich, "A mathematical model for periodic scheduling problems," *SIAM Journal on Discrete Mathematics*, vol. 2, no. 4, pp. 550–581, 1989.

[3] A. Higgins, E. Kozan, and L. Ferreira, "Optimal scheduling of trains on a single line track," *Transportation Research Part B: Methodological*, vol. 30, no. 2, pp. 147–161, 1996.

[4] M. R. Bussieck, T. Winter, and U. T. Zimmermann, "Discrete optimization in public rail transport," *Mathematical Programming*, vol. 79, no. 1-3, pp. 415–444, 1997.

[5] J.-F. Cordeau, P. Toth, and D. Vigo, "A survey of optimization models for train routing and scheduling," *Transportation Science*, vol. 32, no. 4, pp. 380–404, 1998.

[6] A. Caprara, M. Fischetti, and P. Toth, "Modeling and solving the train timetabling problem," *Operations Research*, vol. 50, no. 5, pp. 851–861, 2002.

[7] V. Cacchiani and P. Toth, "Nominal and robust train timetabling problems," *European Journal of Operational Research*, vol. 219, no. 3, pp. 727–737, 2012.

[8] M. Wardman, J. Shires, W. Lythgoe, and J. Tyler, "Consumer benefits and demand impacts of regular train timetables," *International Journal of Transport Management*, vol. 2, no. 1, pp. 39–49, 2004.

[9] A. Ceder, "A procedure to adjust transit trip departure times through minimizing the maximum headway," *Computers & Operations Research*, vol. 18, no. 5, pp. 417–431, 1991.

[10] K. Nachtigall, "Periodic network optimization with different arc frequencies," *Discrete Applied Mathematics*, vol. 69, no. 1-2, pp. 1–17, 1996.

[11] K. Nachtigall and S. Voget, "A genetic algorithm approach to periodic railway synchronization," *Computers & Operations Research*, vol. 23, no. 5, pp. 453–463, 1996.

[12] M. A. Odijk, "A constraint generation algorithm for the construction of periodic railway timetables," *Transportation Research Part B: Methodological*, vol. 30, no. 6, pp. 455–464, 1996.

[13] C. Liebchen, "The first optimized railway timetable in practice," *Transportation Science*, vol. 42, no. 4, pp. 420–435, 2008.

[14] Y. Shafahi and A. Khani, "A practical model for transfer optimization in a transit network: model formulations and solutions," *Transportation Research Part A: Policy and Practice*, vol. 44, no. 6, pp. 377–389, 2010.

[15] X Li and H. K. Lo, "An energy-efficient scheduling and speed control approach for metro rail operations," *Transportation Research Part B: Methodological*, vol. 64, pp. 73–89, 2014.

[16] D. T. Aksu and U. Akyol, "Transit coordination using integer-ratio headways," *IEEE Transactions on Intelligent Transportation Systems*, vol. 15, no. 4, pp. 1633–1642, 2014.

[17] X. Yang, X. Li, Z. Gao, H. Wang, and T. Tang, "A cooperative scheduling model for timetable optimization in subway systems," *IEEE Transactions on Intelligent Transportation Systems*, vol. 14, no. 1, pp. 438–447, 2013.

[18] H. Niu and X. Zhou, "Optimizing urban rail timetable under time-dependent demand and oversaturated conditions," *Transportation Research Part C: Emerging Technologies*, vol. 36, pp. 212–230, 2013.

[19] W. O. Assis, B. E. Milani, and A. Milani, "Generation of optimal schedules for metro lines using model predictive control," *Automatica*, vol. 40, no. 8, pp. 1397–1404, 2004.

[20] V. Guihaire and J. K. Hao, "Transit network design and scheduling: a global review," *Transportation Research Part A: Policy and Practice*, vol. 42, no. 10, pp. 1251–1273, 2008.

[21] T. Albrecht, "Automated timetable design for demand-oriented service on suburban railways," *Public Transport*, vol. 1, no. 1, pp. 5–20, 2009.

[22] E. Hassannayebi, A. Sajedinejad, and S. Mardani, "Urban rail transit planning using a two-stage simulation-based optimization approach," *Simulation Modelling Practice and Theory*, vol. 49, pp. 151–166, 2014.

[23] L. Sun, J. G. Jin, D. H. Lee, K. W. Axhausen, and A Erath, "Demand-driven timetable design for metro services," *Transportation Research Part C: Emerging Technologies*, vol. 46, pp. 284–299, 2014.

[24] H. Niu, X. Zhou, and R. Gao, "Train scheduling for minimizing passenger waiting time with time-dependent demand and skip-stop patterns: nonlinear integer programming models with linear constraints," *Transportation Research Part B: Methodological*, vol. 76, pp. 117–135, 2015.

[25] Y. Wang, T. Tang, B. Ning, TJ van den Boom, and B De Schutter, "Passenger-demands-oriented train scheduling for an urban rail transit network," *Transportation Research Part C: Emerging Technologies*, vol. 60, pp. 1–23, 2015.

[26] Y. Zhu, B. Mao, Y. Bai, and S. Chen, "A bi-level model for single-line rail timetable design with consideration of demand and capacity," *Transportation Research Part C: Emerging Technologies*, vol. 85, pp. 211–233, 2017.

[27] J. Shi, L. Yang, J. Yang, and Z. Gao, "Service-oriented train timetabling with collaborative passenger flow control on an oversaturated metro line: an integer linear optimization approach," *Transportation Research Part B: Methodological*, vol. 110, pp. 26–59, 2018.

[28] Y. Wang, A. D'Ariano, J. Yin, L. Meng, T. Tang, and B. Ning, "Passenger demand oriented train scheduling and rolling stock circulation planning for an urban rail transit line," *Transportation Research Part B: Methodological*, vol. 118, pp. 193–227, 2018.

[29] J. Xie, J. Zhang, K. Sun, S. Q. Ni, and D. Chen, "Passenger and energy-saving oriented train timetable and stop plan synchronization optimization model," *Transportation Research Part D: Transport and Environment*, vol. 98, p. 102975, Article ID 102975, 2021.

[30] Y. Huang, C. Mannino, L. Yang, and T. Tang, "Coupling time-indexed and big-M formulations for real-time train scheduling during metro service disruptions," *Transportation Research Part B: Methodological*, vol. 133, pp. 38–61, 2020.

[31] J. Yin, L. Yang, T. Tang, Z. Gao, and B. Ran, "Dynamic passenger demand oriented metro train scheduling with energy-efficiency and waiting time minimization: mixed-integer linear programming approaches," *Transportation Research Part B: Methodological*, vol. 97, pp. 182–213, 2017.

[32] E. Barrena, D. Canca, L. C. Coelho, and G. Laporte, "Single-line rail rapid transit timetabling under dynamic passenger demand," *Transportation Research Part B: Methodological*, vol. 70, pp. 134–150, 2014.

[33] D. Canca, E. Barrena, E. Algaba, and A. Zarzo, "Design and analysis of demand-adapted railway timetables," *Journal of Advanced Transportation*, vol. 48, no. 2, pp. 119–137, 2014.

[34] D. Chen, S. Li, J. Li, S. Ni, and X. Liu, "Optimal high-speed railway timetable by stop schedule adjustment for energy-saving," *Journal of Advanced Transportation*, vol. 2019, pp. 1–9, Article ID 4213095, 2019.

[35] L. Meng, M. Muneeb Abid, X. Jiang, A. Khattak, and M. Babar Khan, "Increasing robustness by reallocating the margins in the timetable," *Journal of Advanced Transportation*, vol. 2019, pp. 1–15, Article ID 1382394, 2019.

[36] E. Barrena, D. Canca, L. C. Coelho, and G. Laporte, "Exact formulations and algorithm for the train timetabling problem with dynamic demand," *Computers & Operations Research*, vol. 44, pp. 66–74, 2014.

[37] S. Yang, F. Liao, J. Wu et al., "A bi-objective timetable optimization model incorporating energy allocation and passenger assignment in an energy-regenerative metro system," *Transportation Research Part B: Methodological*, vol. 133, pp. 85–113, 2020.

[38] X. Dong, D. Li, Y. Yin, S. Ding, and Z. Cao, "Integrated optimization of train stop planning and timetabling for commuter railways with an extended adaptive large neighborhood search metaheuristic approach," *Transportation Research Part C: Emerging Technologies*, vol. 117, p. 102681, Article ID 102681, 2020.